CHAPTER 3

Unexpected changes of rat cervical spinal cord tolerance caused by inhomogeneous dose distributions

Hendrik P. Bijl, Peter van Luijk, Rob P. Coppes,
Jacobus M. Schippers, Antonius W.T. Konings
and Albert J. van der Kogel

International Journal of Radiation Oncology Biology Physics
2003; 57: 274-281

Abstract

Purpose: The effects of dose-distribution on dose-effect relationships have been evaluated and from this iso-effective doses (ED_{50}) established.

Methods and Materials: Wistar rats were irradiated on the cervical spinal cord with single doses of unmodulated protons (150 MeV) to obtain sharp lateral penumbras, using the shoot through technique which employs the plateau of the depth-dose profile rather than the Bragg peak. Two types of inhomogeneous dose distributions have been administered: (1) two 4 mm fields with 8 or 12 mm spacing between the center of the fields (referred to as split-field) were irradiated with variable single doses and (2) cervical spinal cord was irradiated with various combinations of relatively low doses to a large volume (20 mm) combined with high doses to a small volume (4 mm) (referred to as bath and shower). The endpoint for estimating the dose-response relationships was paralysis of the fore and/or hind limbs.

Results: The split-field experiments (2 x 4 mm) showed a shift in the dose-response curves, giving significant higher ED_{50} values of 45.4 Gy and 41.6 Gy for 8 and 12 mm spacing, respectively, compared with the ED_{50} of 24.9 Gy for the single 8 mm (same total tissue volume irradiated). These values were close to the ED_{50} for a single 4 mm field of 53.7 Gy. The bath and shower experiments showed a large decrease of the ED_{50}'s from 15-22 Gy when compared with the 4 mm single field, even with a bath dose as low as 4 Gy. There were no histological changes found in the low dose bath regions of the spinal cord at post-mortem.

Conclusions: Not only the integral irradiated volume is a determining factor for the ED_{50} of rat cervical spinal cord, but also the shape of the dose distribution is of great importance. The high ED_{50} values of a small region or shower (4 mm) decreases significantly when the adjacent tissue is irradiated with a sub threshold dose (bath), even as low as 4 Gy. The significant shift to lower ED_{50} values for induction of paralysis of the limbs by adding a low dose bath was not accompanied by changes in histological lesions. These observations may have implications for the interpretation of complex treatment plans and normal tissue complication probability in intensity modulated radiotherapy.

Introduction

The spinal cord is a major dose-limiting organ in radiation oncology. Radiation damage to the spinal cord can induce radiation myelopathy with functional deficits. The incidence of radiation myelopathy 5 years after 60 Gy of conventional daily 1.8-2 Gy fractions is 1-5% (1).

The introduction of Intensity Modulated Radiotherapy (IMRT) has lead to dose escalation studies which resulted in increasing tumor doses and equal or lower doses to the surrounding normal tissue. In order to allow a safe increase of tumor dose with acceptable normal tissue toxicity, it is a prerequisite to correctly account for normal tissue responses in the presence of inhomogeneous dose distributions outside the planning target volume (PTV) (2). Hence, for the optimization of the IMRT treatment plans, more data for biological and physical optimization criteria are needed, especially to study the effect of inhomogeneous dose distribution. However, the only data existing describing dose-response relationships and dose-volume effects for the central nervous system are obtained from animal studies (3,4,5,6) after homogeneous irradiation of the spinal cord.

In the present study the issue of inhomogeneous dose distributions was investigated in rat cervical spinal cord with a high precision proton-beam irradiation. The rat cervical spinal cord was irradiated with two types of inhomogeneous dose distributions. In the first group of experiments two 4 mm segments of spinal cord (*split-field*) were irradiated and in the second group of experiments the cervical spinal cord was irradiated with various combinations of relatively low doses to a large volume (*bath*) combined with high doses to a small volume (*shower*). In all the experiments the dose-response relationship for paralysis of fore and/or hind limbs was used as endpoint. The dose-response relationships were compared with recent data obtained after homogeneous high precision proton-beam irradiation of variable lengths of the rat cervical spinal cord (3).

Materials and methods

Animals

Male Wistar rats weighing 200-250 grams were used in the present study. After irradiation the animals were housed two per cage and provided with food and water ad libitum. All experiments were carried out in agreement with the Netherlands Experiments on Animals Act (1977) and the European Convention for the Protection of Vertebrates used for Experimental Purpose (Strasbourg, 18.III.1986).

The animals were checked for development of paralysis of fore and hind limbs regularly, at least twice weekly. Animals were scored as responders when they showed signs of paralysis of the fore and or hind limbs. The time from irradiation to the time of paralysis is referred to as the latent period. Rats dying without neurological symptoms were recorded as intercurrent deaths (n=3). Only animals with paralysis were recorded as responders.

When paralysis had developed, the rat was killed and the spinal column was removed and fixated in formalin 4% for at least 24 hours. After fixation the spinal column was decalcified in a mixture of sodium formiat 8% and formic acid 40% for a period of 7 days after which the spinal cord was processed using a standard paraffin-embedding method for routine Hematoxylin and Eosin (H&E) staining. The blocked spinal cord tissue was sectioned at 4 μm and mounted on microscopic slides.

The cut-off time to establish the endpoint of paralysis due to white matter necrosis was set at 210 days in all experiments. This is based on the rat spinal cord model (5) characterized by two distinct pathologies, selective white matter necrosis and late vasculopathies. The selective white matter necrosis resulted in paralysis within 210 days whereas late vascular lesions in the white and gray matter were observed after a variable period of at least 8 but generally 12 months or more.

The rats were irradiated with single doses of unmodulated 150 MeV protons from the AGOR (**A**ccelerateur **G**roningen **OR**say) cyclotron of the Kernfysisch Versneller Instituut in Groningen. With this technique a homogeneous dose is

deposited along the beam direction, with a penumbra (80-20% iso-doses) of approximately 1 mm (7). It should be emphasized that the Bragg peak in the depth-dose distribution was not used. Instead the target volume was located at a total depth of 3 centimeters. This irradiation method is usually referred to as shoot through technique. The transversal beam size, defined by a collimator position at 15 cm in front of the rat, determined the length of the irradiated part of the cervical spinal cord. The dose rate was in the range of 15-20 Gy/min. The administered doses were monitored during the experiments.

Dose distribution types

Split-field irradiation (Fig. 1A): Two 4 millimeter segments (2 x 4 mm) of cervical spinal cord were irradiated with variable doses (Table 1). The spacing or gap between the centers of the 4 mm segments was 8 or 12 mm. The dose in the spinal cord tissue between the 4 mm segments was less than 5 % of D_{max}.

Symmetrical bath and shower experiments (Fig.1B): Twenty millimeters of cervical spinal cord was irradiated with variable sub threshold doses (referred to as *bath*). These sub threshold or *bath* doses by themselves do not induce paralysis after irradiation of the cervical spinal cord. One 4 mm segment was irradiated with variable single doses (referred to as *shower*) and superimposed on the 20 mm bath. This 4 mm field was located at the fourth cervical vertebra (C4), in the center of the bath. Hence, both adjacent sides of the high dose shower volume were irradiated with sub threshold doses and therefore this experiment was referred to as *symmetrical bath and shower* experiment. The variable bath and shower doses are listed in Table 1.

Asymmetrical bath and shower experiments (Fig.1C): One 12 mm segment (*bath)* was irradiated with a single fraction of 18 Gy. This 12 mm *bath* was located adjacent to the cranial or caudal border of the 4 mm *shower* segment. This 4 mm segment or *shower* was irradiated with variable single doses and superimposed on the 12 mm segment (Table 1) at the level of C4. Since only one adjacent side relative to the shower was irradiated, this experiment was referred to as a *asymmetrical bath and shower* irradiation.

For the dose in the high dose region or *shower* we refer to the total dose received in this region.

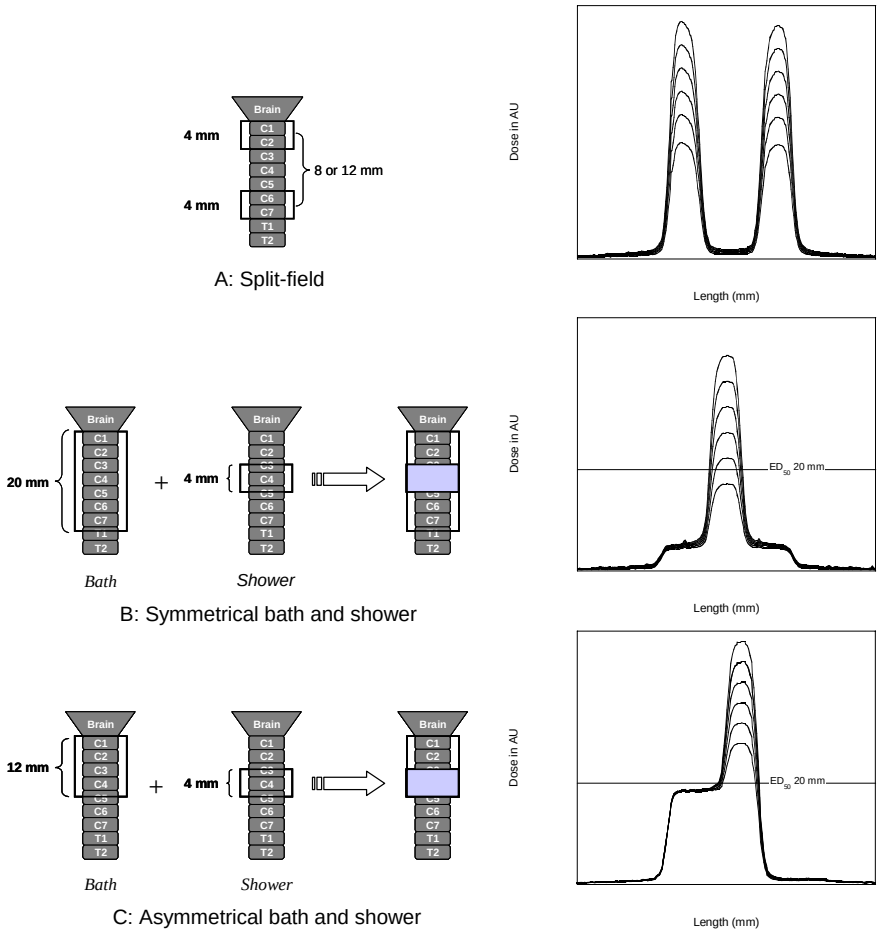

Figure 1. Schematic outline of the present experiments. The rat cervical spinal cords with the used combination of irradiation fields are depicted on the left. The corresponding dose distributions are shown on the right: s*pit-field* (A), *symmetrical* bath and shower (B) and *asymmetrical* bath and shower (C).

Table 1. Overview of the experiments

Experiment	Bath Dose (Gy)	Dose (Gy) per group *(number of responders/irradiated rats)*
Split-field *(2x4 mm)*		
8 mm spacing:	-	**25** *(0/6)*; **30** *(0/6)*; **35** *(0/6)*; **40** *(1/6)*; **45** *(4/6)*; **50** *(4/6)*
12 mm spacing:	-	**25** *(0/5)*; **30** *(0/6)*; **35** *(1/6)*; **40** *(2/6)*; **45** *(4/6)*; **50** *(5/5)*
Symmetrical *bath & shower*	4	**30** *(0/4)*; **32** *(1/10)*; **34** *(0/6)*; **35** *(0/6)*; **36** *(4/12)*; **38** *(2/6)*; **40** *(13/18)*; **42** *(4/4)*; **44** *(9/10)*; **45** *(3/6)*; **46** *(4/4)*; **48** *(6/6)*; **50** *(6/6)*; **52** *(5/5)*; **55** *(6/6)*; **60** *(6/6)*
	12	**25** *(0/6)*; **28** *(0/6)*; **30** *(0/6)*; **32** *(5/6)*; **35** *(3/6)*; **36** *(4/6)*; **40** *(12/12)*; **44** *(6/6)*; **45** *(6/6)*; **48** *(5/5)*; **50** *(5/5)*
	18	**25** *(0/5)*; **30** *(3/5)*; **35** *(4/6)*; **40** *(6/6)*; **45** *(5/5)*; **50** *(4/4)*
Asymmetrical *bath & shower*		
Shower in caudal end of bath:	18	**28** *(1/5)*; **32** *(3/7)*; **36** *(3/6)*; **40** *(1/6)*; **44** *(5/6)*; **48** *(5/5)*
Shower in cranial end of bath:	18	**28** *(0/5)*; **32** *(1/6)*; **36** *(2/6)*; **40** *(5/6)*; **44** *(4/5)*; **48** *(3/4)*

Irradiation Protocol

After induction anesthesia (2.5% Isoflurane and 0.75 l/min O_2 for 10 minutes), six rats at a time were placed vertically at equal distance in a Perspex frame with the head fixed. During the irradiation the anesthesia was maintained with a mixture of 2.5% Isoflurane, 0.5 l/min O_2 and 1 l/min N_2O.

The rats were irradiated on the cervical region (C1-T2) of the spinal cord. The center of the proton beam coincided with an alignment laser, used to position the spinal cord. In all experiments, the fourth cervical vertebra was positioned in the center of the field. When irradiation of one animal was complete, the frame was shifted by remote control until the next rat was in position. In the bath and shower experiments, the time between application of the bath dose and the shower dose varied from 11-19 minutes. There was no specific order in applying the bath or shower doses.

Dosimetry

During irradiation the dose was monitored by a parallel plate ionization chamber mounted in front of the collimator. The relation between the number of monitor units (MU) and the dose in the target was calibrated with a standard reference ionization chamber (Farmer type, PTW30001). For this calibration a sufficiently large (∅ = 7 cm) irradiation field was used to ensure the prescribed homogeneous irradiation of the Farmer chamber. The Farmer chamber was surrounded by polyethylene to account for the tissue and frame material around the spinal cord.

The small collimator apertures used in the present study induced distortions, resulting in a reduction of the dose per MU of up to 20%. Therefore, for all fields the dose distribution in the two transversal dimensions have been measured by means of a fluorescent screen, positioned at the beam exit-side of a 3 cm sheet of polyethylene simulating the depth in tissue. It has been shown that the light output of this screen is a very accurate measure of the dose (8). The spatial resolution is sufficient to correctly measure the smallest dose distribution (0.22 mm standard deviation) (7). The light output of the screen was calibrated against the Farmer chamber in the ∅ 7 cm field.

Data analysis

Dose-response curves were constructed by probit-analysis. For the statistical analysis we used the SPSS 9.0 (SPSS Inc.) for Windows (Microsoft Corporation). Graphics were constructed with KaleidaGraph (Synergy software).

Results

Histology

The histology of the cervical spinal cord of the paralyzed rats showed diffuse white matter necrosis in the high dose shower segment (Fig. 2). The unirradiated tissue from the *split-field* irradiations and the low-dose irradiated tissue from the *bath* volume that received doses up to 18 Gy, showed no signs of histological

damage. These results are in agreement with previous histology studies where tissue irradiated with doses less than 20 Gy showed no discernible changes by light microscopy (5).

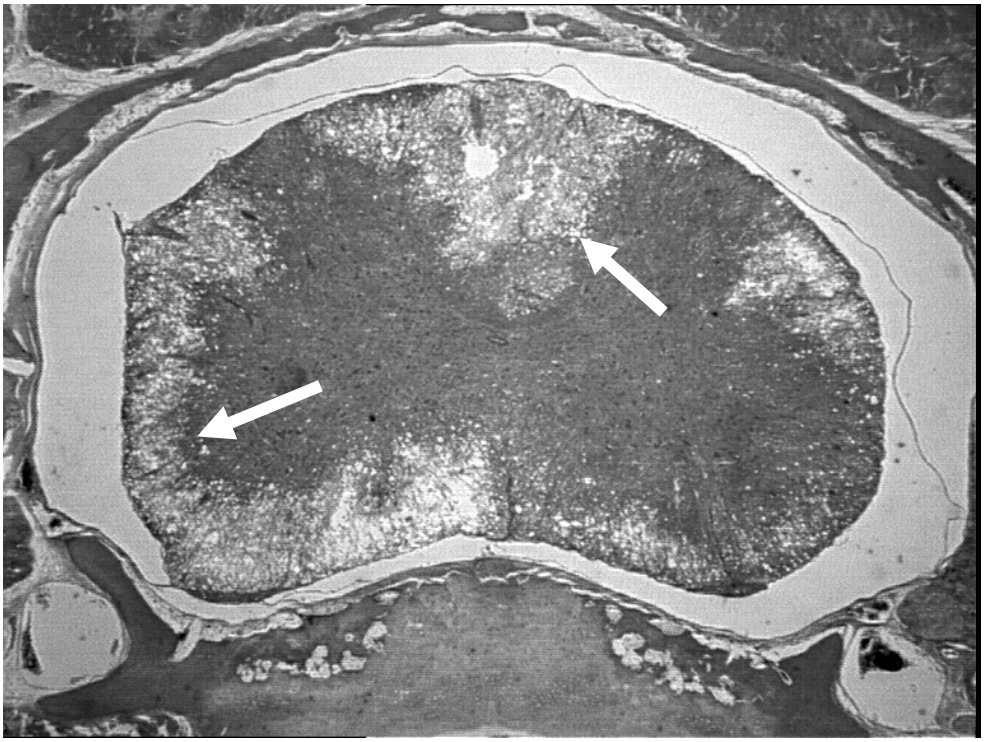

Figure 2. Transverse section of the rat cervical spinal cord at the level of the high-dose 4 mm shower (hematoxylin and eosin stained). Extensive white matter necrosis is predominantly seen in the right ventrolateral column and dorsal tract of the white matter (see white arrows). The rat developed hind and fore limb paralysis after 163 days after irradiation with 50 Gy.

Dose-response relationship

Split-field (2 x 4 mm) (SF): The dose-response curves of the *split-field* (2 x 4 mm) irradiation experiments (Fig. 1A) are shown in Fig. 3 together with 4 and 8 mm single field data as published recently (3). These results are compared with the dose-response curves for the homogeneously irradiated 8 mm single field since the same total irradiated volume is included. The dose-response curves for the 2 x 4

mm split-field are shifted to the right compared with the single 8 mm field indicating ED_{50} values of 45.4 and 41.6 Gy, compared with 24.9 Gy for the 8 mm field (Table 2). The higher ED_{50} values are significantly different from those obtained for the homogeneously irradiated 8 mm single field and closer to the value of 53.7 Gy for the homogeneously irradiated single 4 mm field (Table 2).

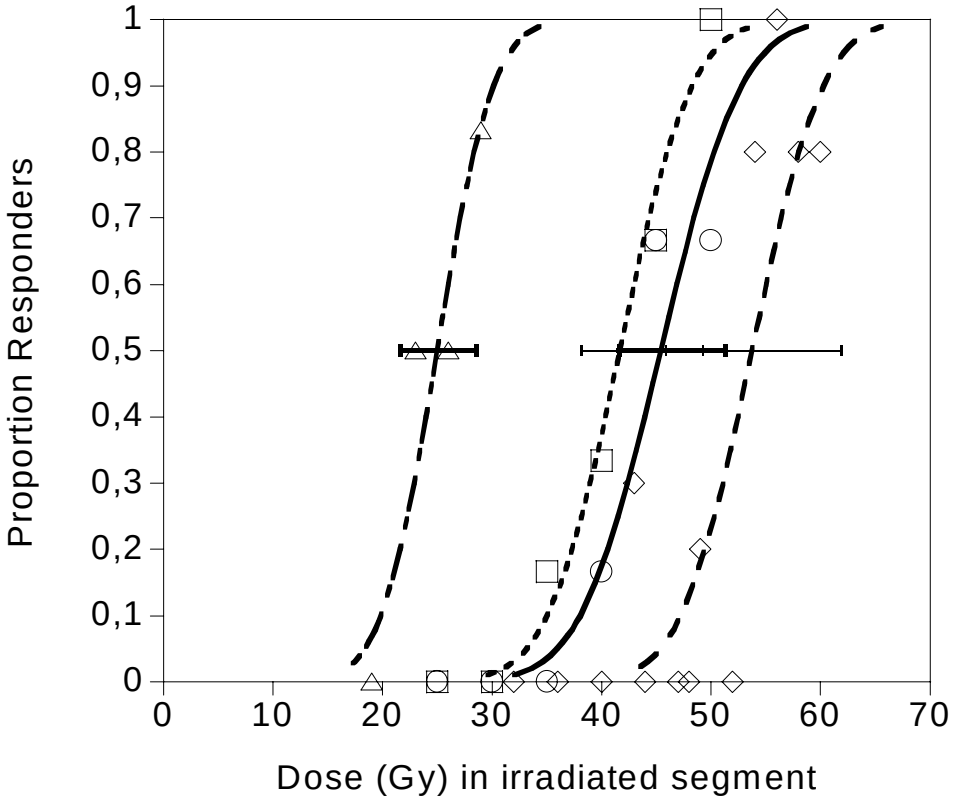

Figure 3. Dose-response curves for paralysis after *split-field irradiation* (squares: 12 mm spacing; circles: 8 mm spacing) compared with homogeneous single field irradiations of 4 mm (diamonds) and 8 mm (triangles) (3). Error bars: 95% confidence intervals.

Table 2. The ED_{50} values of split-field, symmetrical and asymmetrical inhomogeneous irradiation experiments compared with ED_{50} values of 4 mm and 8 mm homogeneously irradiated single fields.

Experiment	Bath Dose (Gy)	ED_{50} (Gy)	95% C.I.
Split-field (2x4 mm)			
8 mm spacing:	-	45.4	40-50
12 mm spacing:	-	41.6	38-46
Symmetrical *bath & shower*	4	39	37-40
	12	33.4	32-35
	18	31.3	26-35
Asymmetrical *bath & shower*			
Shower in caudal end of bath:	18	37.2	30-44
Shower in cranial end of bath:	18	38.4	34-43
Homogeneous irradiation without bath			
(from reference (3))			
4 mm single field:	-	53.7	49-62
8 mm single field:	-	24.9	22-29
20 mm single field:	-	20.4	-

Symmetrical bath and shower (SBS): The dose-response curves for the *symmetrical bath and shower* irradiations (Fig. 1B) are shown in Fig. 4 and compared with the dose-response curve for a homogeneously irradiated 4 and 20 mm single fields (3). The dose-response curves obtained for the *SBS* irradiations show a large shift to the left. A remarkable observation is the unexpectedly large shift to the left of the 4 mm single field dose-response curve by applying a bath dose of only 4 Gy, showing an ED_{50} value of 39 Gy, compared with 53.7 Gy for the 4 mm single field (Fig. 4 A). A further increase of the bath doses to 12 (Fig. 4 B) and 18 Gy (Fig. 4 C) results in a further but relatively smaller decrease to ED_{50}'s of 33.4 and 31.3 Gy, respectively (Table 2). The ED_{50} value for the 4 Gy bath irradiation is

significantly different from the ED_{50} value of the homogeneously irradiated 4 mm single field as well as for the ED_{50} values of the 12 Gy and 18 Gy bath doses.

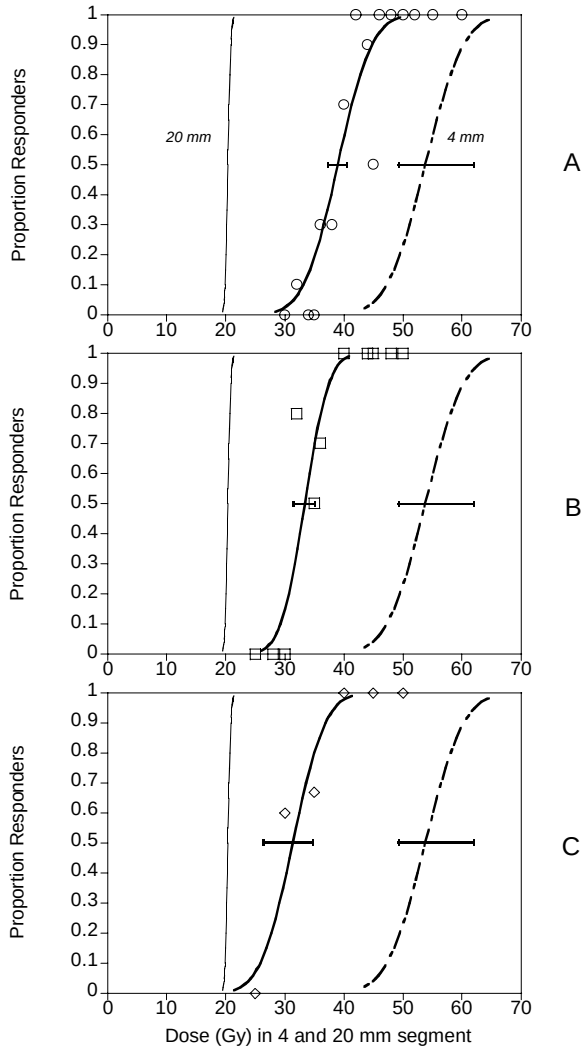

Figure 4. Dose-response curves for paralysis after symmetrical bath and shower irradiation compared with homogeneously irradiated 4 and 20 mm single fields (3). The three graphs show the impact of a 4 Gy (circles), 12 Gy (squares) and 18 Gy (diamonds) bath dose on the dose-response relationship of the 4 mm single field. Error bars: 95% confidence intervals.

Asymmetrical bath and shower (ABS): The dose-response curves of the *asymmetrical bath and shower* irradiations are shown in Fig. 5 and compared with the dose-response curve for the homogeneously irradiated 4 and 20 mm single fields. The addition of the 18 Gy bath cranial or caudal to the 4 mm shower resulted in a shift to the right of the dose-response curve for the 4 mm single field. The ED_{50} values for the ABS were 30.7 and 28.5 % less than the ED_{50} for the 4 mm single field (from 53.7 Gy to 37.2 and 38.4 Gy). This effect is less pronounced than in the symmetrical 18 Gy bath experiment (Table 2). However, a symmetrical 4 Gy bath had the same effect on the 4 mm single field dose-response curve as the ABS. The location of the bath relative to the shower is not of influence on the dose-response curves of the *asymmetrical bath and shower* irradiations.

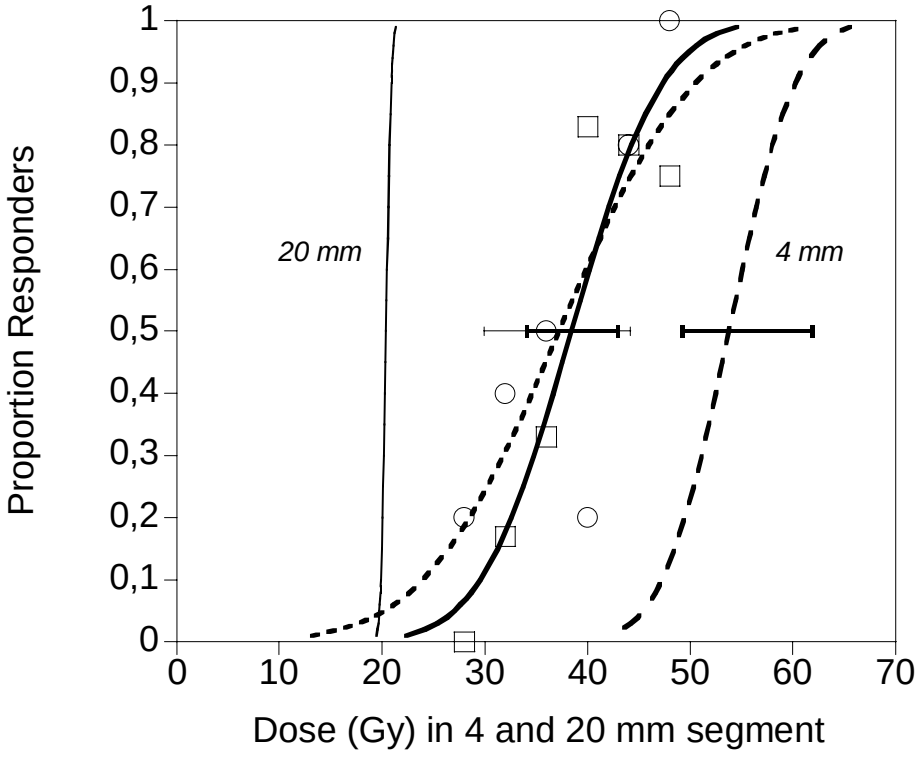

Figure 5. The dose-response curves for paralysis after asymmetrical bath and shower irradiation compared with homogeneously irradiated 4 and 20 mm single fields (3). Caudal bath: circles; cranial bath: squares. Error bars: 95% confidence intervals.

Discussion

In most studies of dose-volume effects the shape of the irradiated volume and the dose distribution are not taken into account. Therefore, we used split-field (Fig. 1A) and bath and shower (Fig. 1B and 1C) irradiation experiments as a model for studying the effect of inhomogeneous dose distributions on dose-volume effects in the rat cervical spinal cord.

The split-field (2 x 4 mm) (Fig. 1A) experiments show that the dose-response relationships are significantly different from the homogeneously irradiated 8 mm single field although the total irradiated volume is the same in both conditions. The ED_{50} values for the *split-field* irradiation are closer to the ED_{50} values obtained for a 4 mm single field (3). This experiment shows that in small fields the response is determined by the volume of a discrete segment, rather than the total irradiated volume. These results cannot be explained by the existing NTCP models (9), since these models do not distinguish between two-segment and single-segment irradiation of the same combined length. This clearly shows the influence of unirradiated tissue adjacent to the irradiated small high dose volume on the tolerance of the small volume. The mechanisms that are involved are not fully understood. It is known that tissues with a high cellular migratory capacity exhibit a steep increase in ED_{50} values at very small volumes, whereby repopulation by migration explains why it is the absolute field size rather than the relative field size that matters for anatomical/structural radiation damage (10). This phenomenon can be observed in tissues like skin and intestinal epithelium (11). In pig skin a rise of the ED_{50} value for moist desquamation is observed when sources less than 22.5 mm are used (10). For the mouse colorectal epithelium, complete re-epithelialiation occurred after 32 Gy when delivered to lengths of less than 5-10 mm but not more than 20 mm, the threshold for consequential obstruction (11). In the rat spinal cord a limited migration distance of glial progenitor cells of 2 mm has been reported (12). The ED_{50} values for the rat cervical spinal cord show a steep rise when lengths shorter than 8 mm are irradiated (3, 4,13). Migration of progenitor cells to depleted segments could be the explanation for the increase of

the ED_{50}s when exposing segments shorter than 8 mm. Hinks et al showed that a single dose of 40 Gy to a 7 mm segment of rat thoracic spinal cord almost completely depleted the oligodendrocyte progenitor cell (OPC) population (14). This depleted segment was repopulated slowly to normal levels by OPCs from flanking unirradiated areas (15). In the asymmetrical experiment, one of the flanking areas is irradiated with a single dose of 18 Gy and the OPC population in this irradiated segment will be compromised. From literature it is known that the surviving OPC fraction is 50-60% after a 15 Gy single dose irradiation (16). The compromised adjacent bath region may be the cause of an incomplete repopulation of the 4 mm shower segment resulting in a decrease of the ED_{50}s. If migration of repopulating cells plays a role in the repair of radiation induced damage, the present asymmetrical bath and shower irradiations (Fig. 1C) show that there seems to be no preferential direction of migration (cranio-caudal or caudo-cranial) since there is no significant difference between the dose-response curves for the asymmetrical bath and shower irradiations.

In symmetrical bath and shower experiments (Fig.1B) the most unexpected observation was the approximate 15 Gy decrease in the ED_{50} value caused by a bath dose of only 4 Gy. Increasing the bath dose to 12 and 18 Gy, augmented the effect reducing the ED_{50} values by as much as 20-22 Gy (Fig. 6). An important conclusion from these experiments is that a low dose to the tissue surrounding a high dose region, may have a major influence on the tolerance dose of the high dose region.

Recent clinical studies on late rectal bleeding after conformal radiotherapy of prostate cancer showed that there is a correlation of rectal bleeding with volumes exposed to intermediate doses (40-50 Gy) (17). This may indicate that when extensive volumes receiving intermediate doses surround high dose regions, the ability of this surrounding tissue to aid in the tissue repair of a central injury may be inhibited. This is supported by the observations in the present bath and shower (Fig 1B and 1C) experiments.

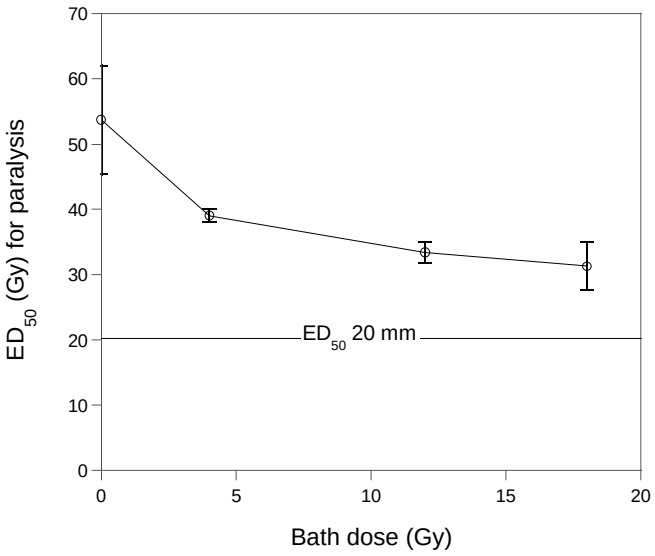

Figure 6. ED_{50} values of the symmetrical bath and shower experiments. The ED_{50} value of the homogeneous single 4 mm field irradiation is set as 0 Gy bath dose. The horizontal line represents the ED_{50} value (20.4 Gy) of a homogeneous single 20 mm field irradiation. Error bars: 95% confidence intervals.

Classically, the pathogenesis of white matter necrosis has been considered as a manifestation of a reduced number of surviving clonogens of either vascular or parenchymal target populations (18). Morris et al. showed in boron neutron capture therapy experiments that endothelial cells were the most likely critical target population in the pathogenesis of white matter necrosis (19). However, based on the classical pathogenesis theory of white matter necrosis with vascular and/or parenchymal cells as targets, the present large decrease of the ED_{50} values cannot be explained. Recent advances in cell biology have shown that growth factors and cytokines are involved in the pathogenesis of radiation induced injury of the central nervous system (CNS) (18, 20). After irradiation of mouse brain, proinflammatory cytokines like tumor necrosis factor α and interleukin 1 (TNF-α and IL-1) are implicated in the pathogenesis of central nervous system damage (21,22). Nieder et al. observed that growth factors can modulate the latent period and the incidence of radiation myelopathy in the rat cervical spinal cord depending on the growth factors and timing of administration (23, 24). From the literature, it

is also known that the cytokine level can influence cells both within and adjacent to the irradiated tissue (18). This out of field effect might play a role in the bath and shower experiments of this study.

The present study shows the impact of differences in dose distribution on the tolerance dose of healthy tissue. The large deviations from model predictions used in standard treatment planning protocols necessitate more research on the dose-response relationship of normal tissues and especially on shape dependence. With the introduction of conformal radiotherapy and IMRT, dose distributions in healthy tissue are more inhomogeneous compared with conventional radiotherapy. The split-field irradiation experiments show that it may be advantageous to distribute the dose in healthy tissue over small volumes embedded in non-irradiated tissue, compared to large contiguous volumes receiving a moderate dose. It should be noted that the present data are the results of single dose irradiations and that extrapolation to fractionated dose delivery may change the observed volume effects. Currently a study on fractionation effects on the dose-response relationships of inhomogeneous dose distributions is in progress. The results presented may be of influence for the planning of treatments involving only a few fractions or in single fraction treatments like radiosurgery.

Conclusions

Not only the irradiated volume is a determining factor of the tolerance dose of rat spinal cord tissue, but especially the shape of the dose distribution is of importance. The high tolerance doses observed for small regions (shower) decrease significantly when the adjacent tissue is irradiated with a sub threshold dose (bath). The low bath doses do not cause structural tissue damage as detected by light microscopy in histology sections.

These results may have implications for the interpretation of complex treatment plans and normal tissue complication probability (NTCP) in intensity modulated radiotherapy (IMRT).

References

1. Fowler JF, Bentzen SM, Bond SJ, et al. Clinical radiation dose for spinal cord: the 1998 international questionnaire. Radiother Oncol 2000;55:295-300.
2. Yorke ED. Modeling the effects of inhomogeneous dose distributions in normal tissues. Semin Radiat Oncol 2001;11:197-209.
3. Bijl HP, Van Luijk P, Coppes RP, et al. Dose-volume effects in the rat cervical spinal cord after proton irradiation. Int J Radiat Oncol Biol Phys 2002;52:205-211.
4. Hopewell JW, Morris AD, Dixon BA. The influence of field size on the late tolerance of the rat spinal cord to single doses of X rays. Br J Radiol 1987;60:1099-1108.
5. Van der Kogel AJ. Late effects of radiation on the spinal cord. Rijswijk: Radiobiological Institute TNO; 1979.
6. Van der Kogel AJ. Central nervous system radiation injury in small animal models. In: Gutin, P. H., Leibel, S. A., Sheline, G. E., editors. Radiation injury to the central nervous system. New York: Raven Press, Ltd.; 1991. p. 91-111.
7. Van Luijk P, Van't Veld AA, Zelle HD, et al. Collimator scatter and 2D dosimetry in small proton beams. Phys Med Biol 2001;46:653-670.
8. Boon SA, Van Luijk P, Schippers JM, et al. Fast 2D phantom dosimetry for scanning proton beams. Med Phys 1998;25:464-475.
9. Stavreva N, Niemierko A, Stavrev P, et al. Modelling the dose-volume response of the spinal cord, based on the idea of damage to contiguous functional subunits. Int J Radiat Biol 2001;77:695-702.
10. Hopewell JW, Trott KR. Volume effects in radiobiology as applied to radiotherapy. Radiother Oncol 2000;56:283-288.
11. Skwarchuk MW, Travis EL. Volume effects and epithelial regeneration in irradiated mouse colorectum. Radiat Res 1998;149:1-10.
12. Franklin RJ, Gilson JM, Blakemore WF. Local recruitment of remyelinating cells in the repair of demyelination in the central nervous system. J Neurosci Res 1997;50:337-344.
13. Van der Kogel AJ. Dose-volume effects in the spinal cord. Radiother Oncol 1993;29:105-109.
14. Hinks GL, Chari DM, O'Leary MT, et al. Depletion of endogenous oligodendrocyte progenitors rather than increased availability of survival factors is a likely

explanation for enhanced survival of transplanted oligodendrocyte progenitors in X-irradiated compared to normal CNS. Neuropath App Neurobiol 2001;27:59-67.

15. Chari DM, Blakemore WF. Efficient recolonisation of progenitor-depleted areas of the CNS by adult oligodendrocyte progenitor cells. Glia 2002;37:307-313.
16. Hopewell JW, van der Kogel AJ. Pathophysiological mechanisms leading to the development of late radiation-induced damage to the central nervous system. In: Wiegel, T., Hinkelbein, W., Brock, M., Hoell, T., editors. Controversies in neuro-oncology. Basel: Karger; 1999. p. 265-275.
17. Jackson A, Skwarchuk MW, Zelefsky MJ, et al. Late rectal bleeding after conformal radiotherapy of prostate cancer (II): volume effects and dose-volume histograms. Int J Radiat Oncol Biol Phys 2001;49:685-698.
18. Nieder C, Ataman F, Price RE, et al. Radiation myelopathy: new perspective on an old problem. Radiat Oncol Invest 1999;7:193-203.
19. Morris GM, Coderre JA, Whitehouse EM, et al. Boron neutron capture therapy: a guide to the understanding of the pathogenesis of late radiation damage to the rat spinal cord. Int J Radiat Oncol Biol Phys 1994;28:1107-1112.
20. Tofilon PJ, Fike JR. The radioresponse of the central nervous system: a dynamic process. Radiat Res 2000;153:357-370.
21. Ruifrok ACC, McBride WH. Growth factors: biological and clinical aspects. Int J Radiat Oncol Biol Phys 1999;43:877-881.
22. Daigle JL, Hong J-H, Chiang C-S, et al. The role of tumor necrosis factor signaling pathways in the response of murine brain irradiation. Cancer Res 2001;61:8859-8865.
23. Nieder C, Price RE, Rivera RE, et al. Both early and delayed treatment with growth factors can modulate the development of radiation myelopathy (RM) in rats (Abstr.). Radiother Oncol 2000;56 (Suppl. 1): S15.
24. Nieder C, Andratschke N, Price RE, et al. VEGF (Vascular Endothelial Growth Factor) modulates the development of radiation myelopathy (RM) in rats (Abstr.). Int J Radiat Oncol Biol Phys 2001;51:127-128.